SAND2018-11901C

Establishing an RMS von Mises Stress Error Bound for Random Vibration Analysis

David Day, Moheimin Khan, Michael Ross, Brian Stevens

Sandia National Laboratories[1]

P.O. Box 5800 – MS0557

Albuquerque, NM 87185

ABSTRACT

The root mean square (RMS) von Mises stress is a criterion used for assessing the reliability of structures subject to stationary random loading. This work investigates error in RMS von Mises stress and its relationship to the error in acceleration for random vibration analysis. First, a theoretical development of stress-acceleration error is introduced for a simplified problem based on modal stress analysis. Using results from the example as a basis, a similar error relationship is determined for random vibration problems. Finite element analyses of test structures subject to an input acceleration auto-spectral density are performed and results from parametric studies are used to determine error. For a given error in acceleration, a relationship to the error in RMS von Mises stress is established. The resulting relation is used to calculate a bound on the RMS von Mises stress based on the computed accelerations. This error bound is useful in vibration analysis, especially where uncertainty and variability must be thoroughly considered.

KEYWORDS: Acceleration, Error Bound, Random Vibration, RMS von Mises Stress, Uncertainty Quantification

1 INTRODUCTION

Finite element models are used to analyze physical systems of interest and they contain errors that arise due to discrepancies between the approximate model and actual system. The source of error in finite element simulations can be generally attributed to three major factors: data input, physics model, and numerical solution accuracy [1]. When the finite element formulation adequately represents the physics of the problem with sufficient numerical accuracy, data input becomes the main source of error. These input errors are often due to uncertainties in loads, geometry, material properties, or boundary conditions.

In structural analysis, a typical use for finite element analysis (FEA) is to evaluate the response of a system under a loading condition and to make predictions, such as determining a margin using some specific criteria. Oftentimes, the quantity of interest is stress, so any source of data input error will cause an uncertainty in stress and the resulting margin. To accurately assess the failure of the system under consideration, it is important to be able to quantify this error relation.

For a random vibration analysis, loading is in the form of an auto-spectral density, or ASD, which is often determined from test results. The quantities of interest are the root mean square von Mises (VRMS) stress and response acceleration ASD. The VRMS is used to predict the failure of structures subject to probabilistic loads and accounts for the complete frequency response of the structure [2]. Data input error arising from uncertainty in material and system properties affects the resulting stresses and accelerations. The acceleration is an important quantity, since most random vibration tests collect acceleration measurements at several locations in a system. Accelerometer data is often readily available, but the stress state at a specific point in a structure may not be. Thus, it is important to quantitively bound uncertainty and error in stress through the acceleration.

[1]Sandia National Laboratories is a multimission laboratory managed and operated by National Technology and Engineering Solutions of Sandia, LLC, a wholly owned subsidiary of Honeywell International, Inc., for the U.S. Department of Energy's National Nuclear Security Administration under contract DE-NA0003525.

In this work, data input errors are used as perturbations to introduce acceleration error and evaluate the limits of the error in stress. Three different example cases are analyzed. The first case uses the magnitude of the error in acceleration to determine a bound on the modal von Mises stress for a free-free beam. In the second and third cases, two different beams are studied in a random vibration setting. For these problems, the sources of error are perturbations in modulus, density, damping, and length. The random vibration solution uses the method presented in [2], where the VRMS stress is calculated using modal stress and displacement amplitudes. An in-depth theoretical development is discussed and the stress-acceleration error relation for the example problem is studied first, followed by results from the other two cases in a random vibration context.

2 THEORY

The equation of motion for a damped, multi-degree of freedom (MDOF) system under load $\underline{F}(t)$ can be expressed as

$$[m]\underline{\ddot{u}}(t) + [c]\underline{\dot{u}}(t) + [k]\underline{u}(t) = \underline{F}(t) \tag{1}$$

where $[m], [c], [k]$ are the system mass, damping, and stiffness matrices, respectively. In a direct solution, the displacements, $\underline{u}(t)$, are computed by numerically solving the coupled partial differential equations of motion. Modal superposition, used in modal-based methods such as random vibration, takes advantage of the modal degrees of freedom, or modal coordinates, $q_n(t)$, to uncouple the equations using the system mode shapes, ϕ_n, as given in [3]:

$$u_n(t) = \phi_n q_n(t) \tag{2}$$

$$[M]\underline{\ddot{q}}(t) + [\Phi]^T[c][\Phi]\underline{\dot{q}}(t) + [K]\underline{q}(t) = \underline{Q}(t) \tag{3}$$

Here, $[M] = [\Phi]^T[m][\Phi]$ is the modal mass matrix, $[K] = [\Phi]^T[k][\Phi]$ is the modal stiffness matrix, and $\underline{Q}(t) = [\Phi]^T\underline{F}(t)$ is the modal force vector. The displacements are calculated by solving the n uncoupled equations for each $q_n(t)$, which are used to determine the strains and stresses at a given time.

In random vibration problems, the quantities of interest are statistical in nature, so a metric such as the VRMS is used to assess failure. For random vibration of MDOF systems in the time domain, the mean square von Mises stress can be calculated using the modal coordinates and the stress mode shapes of the structure [2],

$$\sigma_{VRMS}^2 = E[p^2(t)] = \sum_{i,j} \Gamma_{ij} T_{ij} = \sum_{i,j} E\left[q_i(t) q_j(t)\right] \Psi_i^{\sigma T} A \Psi_j^{\sigma} \tag{4}$$

Here, $E[p^2(t)]$ is the expected value, or mean, of the square of the von Mises stress, $p(t) = \sigma(t)^T A \sigma(t)$, where $\sigma(t)^T = [\sigma_{xx}\ \sigma_{yy}\ \sigma_{zz}\ \sigma_{yz}\ \sigma_{xz}\ \sigma_{xy}]$. The VRMS is calculated using the modal covariance, $\Gamma_{ij} = E\left[q_i(t) q_j(t)\right]$, the stress modes $\Psi_i^{\sigma T}, \Psi_j^{\sigma}$, and matrix A, defined in [2].

In the frequency domain, the modal coordinate, $q_i(\omega)$, is related to the input loads, $f_j(\omega)$, by the transfer function, $H_{ij}(\omega)$ [2]

$$q_i(\omega) = H_{ij}(\omega) f_j(\omega) \tag{5}$$

From [4], the spectral density matrix of the response, $[S_X(\omega)]$, is calculated from the transfer function and the given spectral density matrix, $[S_F(\omega)]$,

$$[S_X(\omega)] = [H(\omega)][S_F(\omega)][H(\omega)]^{\dagger} \tag{6}$$

This reduces in the case of a single input to

$$[S_X(\omega)] = |H(\omega)|^2 [S_F(\omega)] \tag{7}$$

In the frequency domain, the mean square von Mises stress is given as

$$E[p^2(t)] = \sum_m \sum_n \frac{1}{2\pi} \int_{-\infty}^{\infty} \left[\left(H^{\sigma}(\omega)\right)^{\dagger} A H^{\sigma}(\omega)\right]_{mn} S_{ff}(\omega)_{mn} d\omega \tag{8}$$

Additional steps in determining the above equation for VRMS are given in [2].

2.1 Theoretical Development of Acceleration Error

This section details the theory used in relating the modal stress error and acceleration error.

A model is used to attempt to predict measurements. One assumption is that the model converges to the actual measurements under mesh refinement, so predictions can be made regarding the model errors. These predictions are initially made on a coarse mesh. A fine mesh is also used, which is fine enough that the error is the approximately the difference between the coarse and the fine values. The purpose of this section is to describe the calculation of an error bound for the maximum possible von Mises stress on the fine mesh. The input to the algorithm is:

1. A course mesh and a fine mesh
2. Mode shapes on both meshes
3. Stress mode shapes on the fine mesh
4. A linear interpolation operator called the prolongation (coarse to fine)
5. Fine mesh mass matrix
6. Normal acceleration on the coarse mesh, at some time
7. Bound on the L_2 error in the acceleration at that time

The displacements $u(x,t)$ are approximated by their value on some fine mesh, $u_h(x,t)$. A sufficiently fine mesh is chosen such that $u - u_h$ is much smaller than $u_H - u_h$, where $u_H(x,t)$ is the displacement on the coarse mesh. Similar conditions are required for accelerations and von Mises stress. The next assumption is that the trajectory, $u(x,t)$, accelerations and von Mises stress can be well approximated by the low frequency modal approximation, meaning that the modes appropriately describe the system within a valid frequency range of interest.

2.1.1 Reduction to linear algebra

In this section, some intermediate steps are omitted, so further details are given in Appendix A.

On the fine mesh, the modes are the columns of the mode shape vector, $\Phi^h = [\phi_1^h, \dots]$, defined on the mesh nodes. The displacement, u_h, has modal expansion $u_h(x,t) = \Phi_i^h(x)q(t)$, where $q = [q_1, \dots]$. Similarly, the coarse mesh has $u_H = \Phi_i^H(x)b(t)$, with $\Phi^H = [\phi_1^H, \dots]$, and $b = [b_1, \dots]$. Using the corresponding stress modes, $\Psi^h = [\psi_1^h, \dots]$, defined at element centroids, a stress state associated with the corresponding stress mode can be obtained as

$$\sigma_h(x,t) = \Psi^h(x)q(t) \tag{9}$$

The von Mises stress, σ^v, can be calculated from the deviatoric stress tensor, σ^{dev}, as $\sigma^v = \sqrt{\frac{3}{2}(\sigma^{dev} : \sigma^{dev})}$, where ":" denotes the double dot product. Thus, using the deviatoric stress modes, $\sigma_h^{dev}(x,t) = \Psi^{dev}(x)q(t)$, the von Mises stress can be expressed in modal terms as

$$\sigma_h^v(x,t) = \sqrt{\frac{3}{2}}\|\Psi^{dev}(x)q(t)\|_F$$

The goal is to relate to the (squared) maximum von Mises stress, $\max(\sigma_h^v)^2$, to acceleration error and obtain a bound, δ^2, such that

$$\|\ddot{u}_h - P\ddot{u}_H\|_{L^2}^2 < \delta^2 \tag{10}$$

Here, the error is calculated from the Euclidean or L_2 norm of $\ddot{u}_h - P\ddot{u}_H$, and P is a fine to coarse mesh transfer linear operator called the prolongation.

The solution of the optimization problem is the maximum of the solutions over each element. Eigenvalues connect accelerations and displacements, $\ddot{q} = -\Omega_h^2 q$ and $\ddot{b} = -\Omega_H^2 b$ and rigid body modes can be ignored. Due to $q = -\Omega_h^{-2}\ddot{q}$, there holds $(\sigma_h^v)^2 = \ddot{q}^T X \ddot{q}$ for

$$X = [\chi_{ij}], \qquad \chi_{i,j} = \frac{3}{2}\frac{\psi_i^{dev}}{\omega_i^2} : \frac{\psi_j^{dev}}{\omega_j^2} \tag{11}$$

Here, X is a symmetric matrix with a positive diagonal, composed of the deviatoric stress modes and eigenvalues. The bound on the stress is determined by solving the nonlinear equation (10). Some assumptions are made which explain how, for the purposes of this study, solving the nonlinear equation is relatively easy because several complications do not arise. Details are given in Appendix A.

The basic problem is as follows: for given $\ddot{b}$ on the coarse mesh, to maximize $(\sigma_h^v)^2 = \ddot{q}^T X \ddot{q}$ over all $\ddot{q}$ such that the error in acceleration, $\|\ddot{u}_h - P\ddot{u}_H\|_{L^2}^2 < \delta^2$. This provides an understanding of the relationship between the accuracy in acceleration to the accuracy in stress, and how this bound varies with the state of acceleration on the coarse mesh, $\ddot{u}_H$.

3 ANALYSIS EXAMPLES

FEA was performed for three different example problems and a stress-acceleration error relationship was determined for each case. The error is defined as the percent difference in stress or acceleration from a base model that ideally represents the system. Using the theory presented in the previous section, the first case examines the error bound for an unsupported, or free-free, beam. An acceleration error is imposed and the relation to the maximum modal von Mises stress error is found. The second and third cases involve more practical examples, in which random vibration of a cantilever beam and two-material, joint rectangular beam is considered. Material properties and beam geometry are varied (perturbed) to obtain an error in acceleration that is related to the VRMS error. All analysis was performed using Sandia's in-house finite element code Sierra/SD, along with MATLAB and Python scripts.

3.1 Case 1: Free-Free Beam

Analysis for this problem follows the steps outlined in 2.1, with further details provided in Appendix A. An acceleration is initially applied to all nodes in the coarse mesh and the resulting L_2 error in acceleration is linearly varied from an initial δ_{min}, to $\delta_{min} + 2\|c\|$, which is twice the norm of the initial fine mesh acceleration. For the free-free beam, the maximum modal von Mises stress in the beam was calculated on the fine mesh for different values of this L_2 acceleration error. Stress and displacement mode shapes from 16 calculated modes were used.

The beam material is steel and it is 1 inch (25.4 mm) in diameter and 10 inches (254 mm) in length. The beam was meshed with a total of 1920 8-node, linear hexahedral elements (Hex8) as shown in **Fig. 1**. All stress calculations were done on the fine mesh, with a coarse mesh of 240 elements used to apply the acceleration, as mentioned in 2.1.

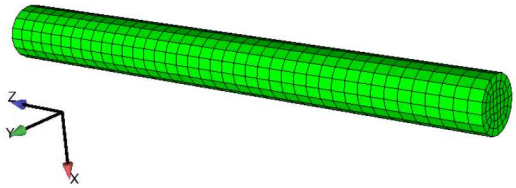

Fig. 1 Free-Free Beam Model: Fine Mesh

The resulting plot in **Fig. 2** shows a linear relationship between the maximum stress error in the model and the acceleration error. The modal von Mises stress distributions[2] for the initial and final stress states are also presented. The acceleration error reached a maximum of 393%, and the error in the von Mises stress was 154%, giving the maximum stress error to acceleration error ratio of 0.392. This error ratio, defined as the maximum percent VRMS error divided by the maximum acceleration percent error relationship provides a measure of the sensitivity of stress error change relative to the acceleration error. It also describes how the errors are bound and is the slope of the percent error plot for a linear relation.

[2] Like the mode shape amplitudes, the mode shape stresses can be arbitrarily scaled, so only the relative values are important here.

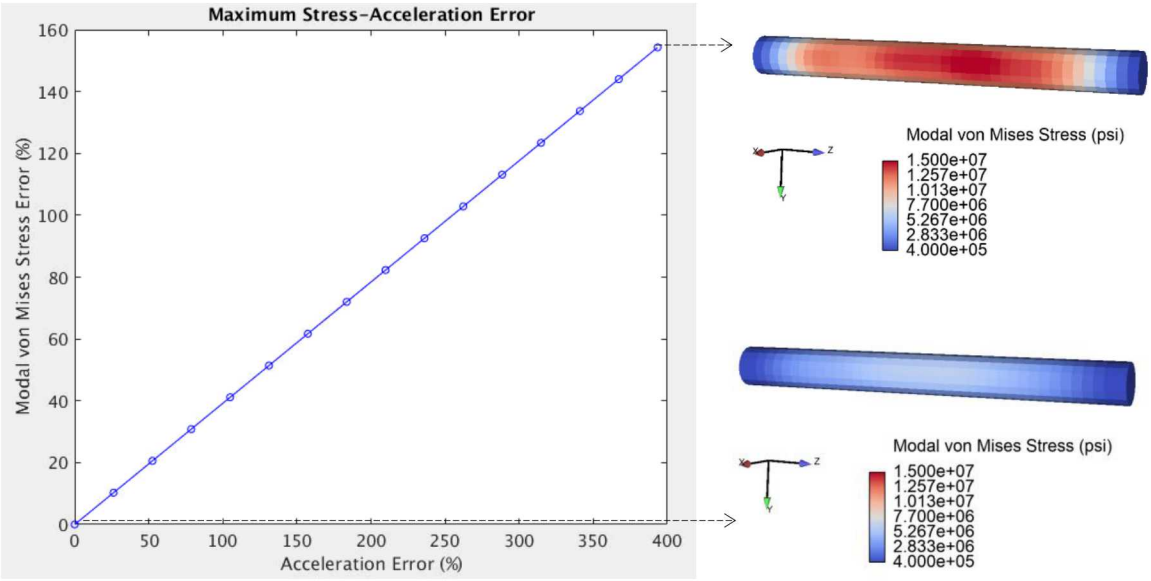

Fig. 2 Stress-Acceleration Error Relationship and Stress Contours for Lowest and Highest Error Values

This relation between the maximum modal stress in the model and the acceleration error is a first step to obtaining a practical error bound. The example case is theoretical, since the accelerations are ideally applied and the resulting modal stresses cannot be used to directly evaluate failure. We are typically interested in more realistic boundary conditions and loading scenarios. Thus, the following sections describe a similar stress-acceleration relationship for beams subject to random vibration loading.

3.2 Case 2: Cantilever Beam Random Vibration

In this example, a cantilever beam is subjected to a 1 g^2/Hz flat random vibration input from 20 to 2000 Hz. The frequency resolution used in the simulations is 0.1 Hz and the response ASD is shown in **Fig. 3**. The loading is applied in the positive Z direction using a concentrated, seismic mass attached with rigid bar elements to the end of the beam. The mass is constrained in all directions except the input to ensure uniform loading.

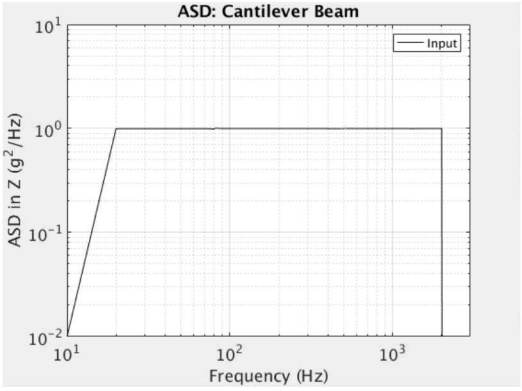

Fig. 3 Random Vibration Input (1 g^2/Hz over 20-2000 Hz; 0.01 g^2/Hz at 10 Hz and 2010 Hz)

To obtain an error in acceleration, the data input values perturbed in the FE simulations were the material and geometric properties, or model parameters. The modulus of elasticity, density, damping ratio (percent of critical), and length were the selected parameters, and each was independently increased by 1% per simulation with a total of 20 simulations per parameter. As one parameter is varied, the others are fixed to a nominal value. The output RMS acceleration in the Z-direction (AZRMS) was studied at two different nodes (points) on the mesh and the average VRMS of the Hex8 elements sharing the points was obtained. For this problem, the locations of the points were the same for each simulation except for the length perturbation, where the distance from the beam end and distance between points was held constant.

The resulting absolute value in VRMS error was plotted versus the absolute value of the AZRMS error. The error for each simulation was calculated using the following equation (12).

$$\% \, Error^{n}_{a_{rms}} = \frac{100|a^{n}_{rms} - a^{0}_{rms}|}{a^{0}_{rms}} \tag{12}$$

Here, a^{0}_{rms} is the RMS value at a selected point for the initial, unperturbed model and a^{n}_{rms} is the RMS value at the same point for the n^{th} perturbed model, where n ranges from 1 to 20 and each subsequent n is a 1% increase in one of the parameters. The same calculation was also done using the maximum values of VRMS and AZRMS over the entire model.

The cantilever beam dimensions are 1 inch (25.4 mm) by 2 inches (50.8 mm) by 20 inches (508 mm) and the material is aluminum. A stress refinement study was initially performed and the final model consists of approximately 160,000 Hex8 elements. **Fig. 4** below shows the beam model.

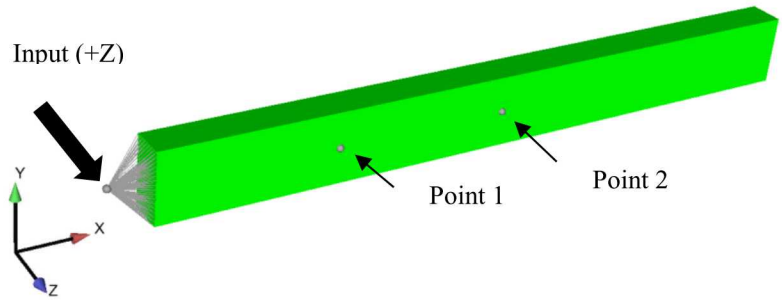

Fig. 4 Cantilever Beam Model with Coordinate System, Input, and Point Location

The response ASD at the two points of interest and the relevant mode shapes for the unperturbed, base model are shown in **Fig. 5** below. The three bending modes about the Y axis are exaggerated for visualization purposes.

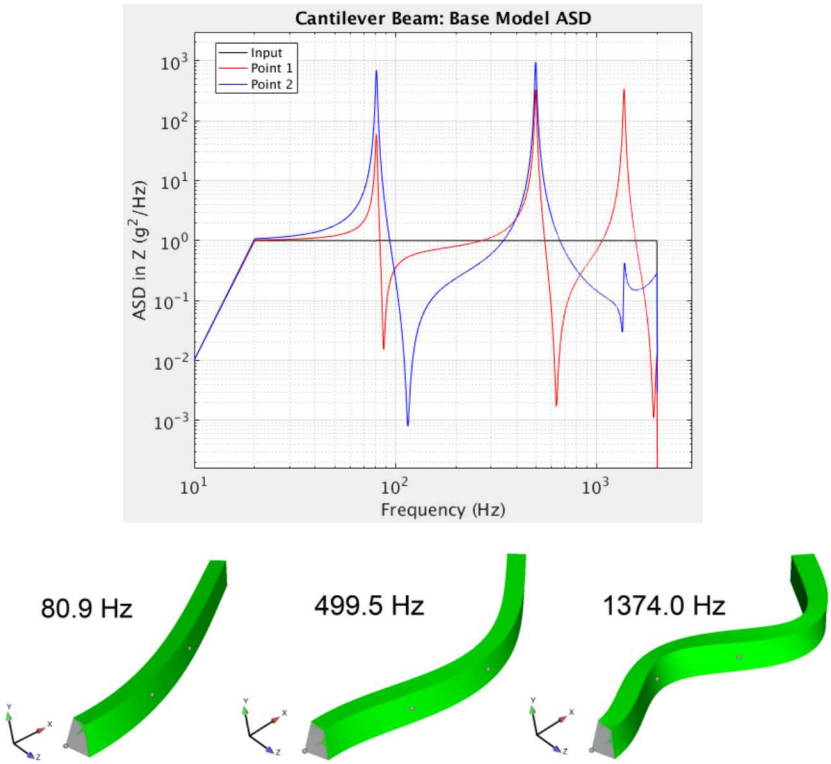

Fig. 5 Cantilever Beam: Base Model Response ASD and Contributing Modes

Plots of the error in VRMS and AZRMS are presented for each of the parameter perturbation studies: modulus of elasticity, damping, density, and length. In addition, the maximum VRMS stress error for each model was plotted against the maximum AZRMS error to obtain an error bound similar to **Fig. 2** in the previous section. A table summarizing the range of maximum values is also given at the end of the section.

For the change in modulus, a one-to-one linear relationship was observed at both points and for the maximum values, as presented in **Fig. 6**. A perturbation in damping also resulted in a direct linear relationship; this was expected for uniform modal damping, so the plots are not shown here and are given in Appendix B. The density relationship in **Fig. 7** also was also linear, while the length perturbation exhibited some nonlinearity[3], which is especially prevalent in the Point 2 plot in **Fig. 8.** After the 16th simulation, there is a turning point in the relation at which the acceleration error decreases while the stress error continues to increase. In addition, the other two length plots look linear initially, but start behaving nonlinearly as the acceleration error increases.

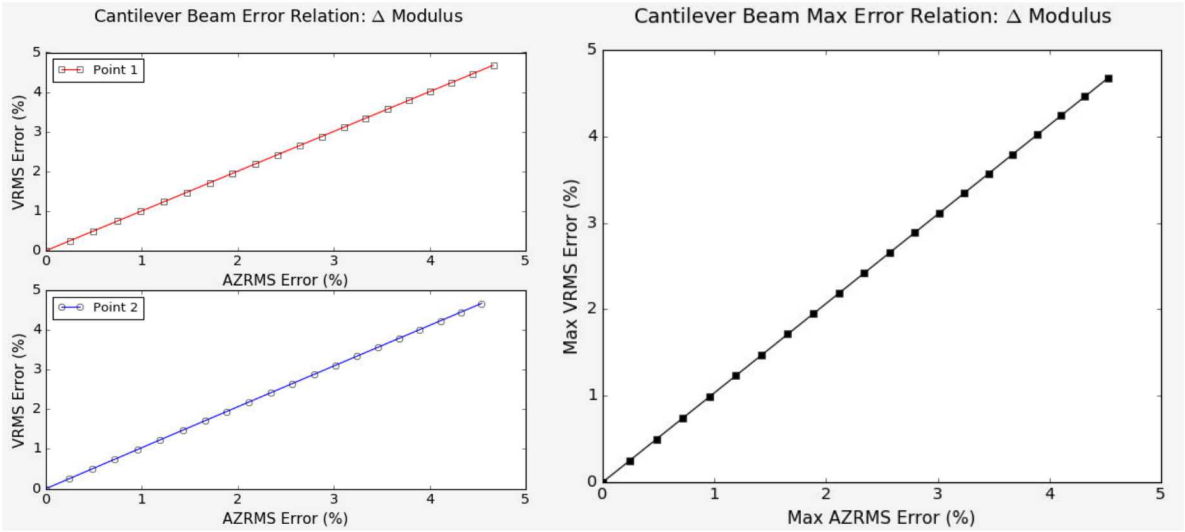

Fig. 6 Cantilever Beam: Effect of Modulus Change on Stress-Acceleration Error Relation, Selected Points and Maximum

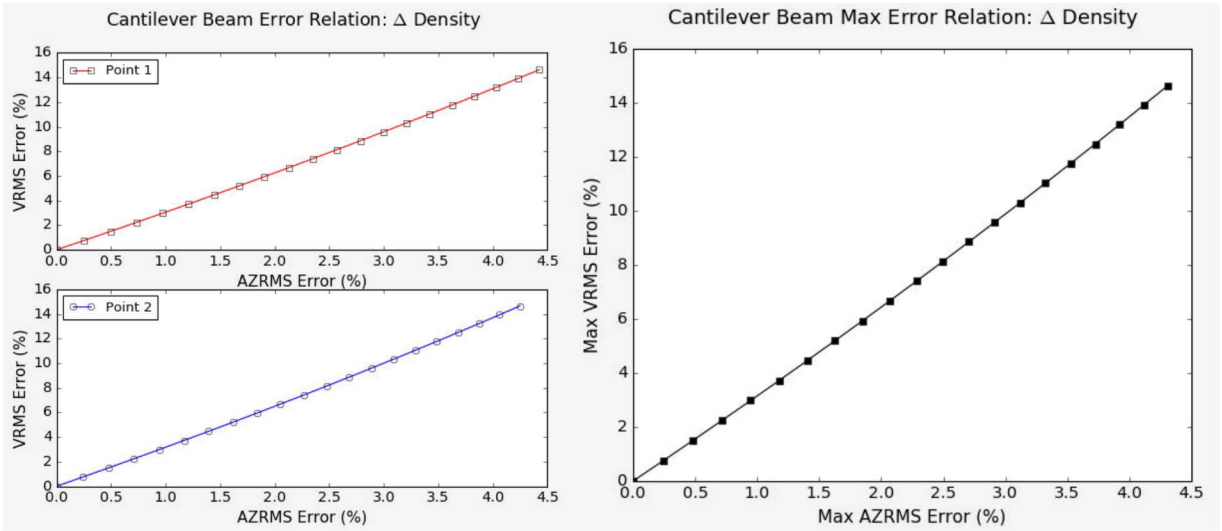

Fig. 7 Cantilever Beam: Effect of Density Change on Stress-Acceleration Error Relation, Selected Points and Maximum

[3] All results are for a linear elastic constitutive model and no frictional effects are considered, so the term "nonlinear" is used in the context of describing the relationship between the errors.

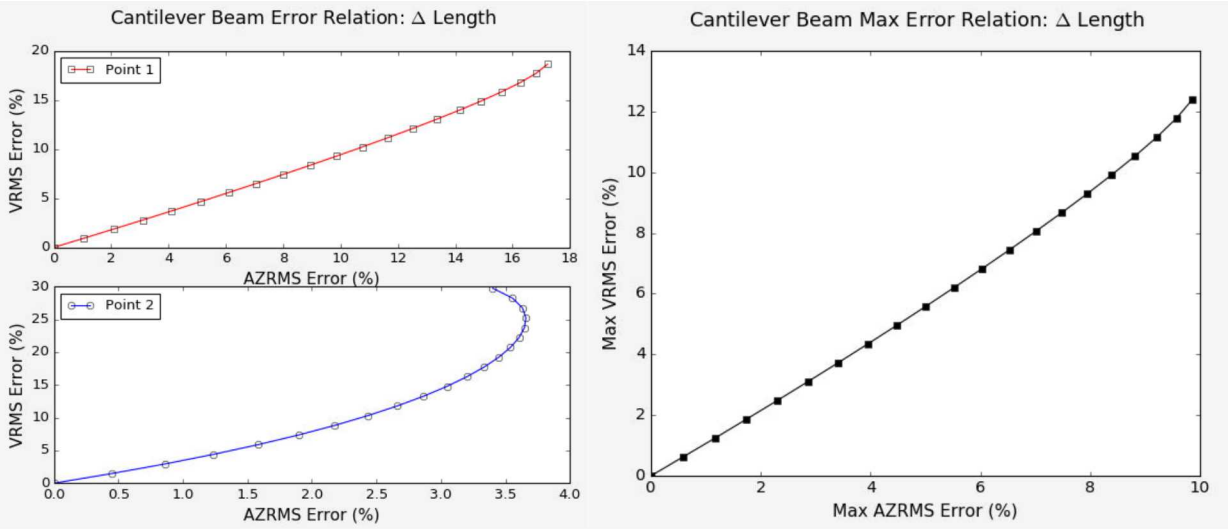

Fig. 8 Cantilever Beam: Effect of Length Change on Stress-Acceleration Error Relation, Selected Points and Maximum

To further investigate possible sources of this nonlinear error relationship, the ASD at Point 2 was plotted for each of the 20 length perturbation simulations. The first plot in **Fig. 9** indicates that a fourth mode starts entering the 20 to 2000 Hz frequency range once the beam length is increased past a certain point. In addition, the response due to the mode initially at 1374 Hz starts to increase well beyond the input level. These two factors suggest that the changing error relationship in the Point 2 plot of **Fig. 8** is caused by the influence of the new mode and the increased response of an existing mode. This significant change in modes and frequencies disrupts the initially linear error relation. On the other hand, the response ASD for the modulus perturbations shown in the second plot of **Fig. 9** demonstrates consistency in the modes and small changes across all 20 simulations, leading to the error relation shown previously in **Fig. 6.**

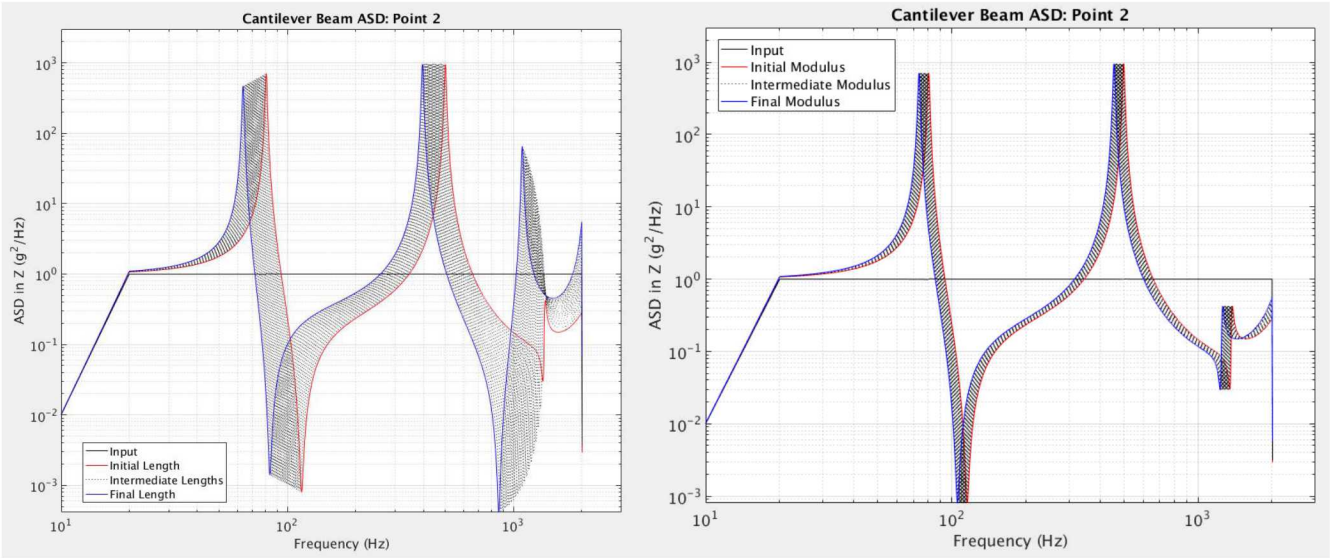

Fig. 9 Cantilever Beam: Complete Range of Response ASD for Length (left) and Modulus (right) Perturbations

A summary of the range of stress-acceleration error and the error ratios is given in **Table 1**. The range of stress values is also listed for reference. The data presented in the table is for the error in the maximum value at any point in the model. This is distinct from the maximum error for a single point in model, but similar values can also be found at the individual points.

Table 1 Cantilever Beam: Maximum Value Error Summary

Perturbation	VRMS Range (psi / MPa)	Maximum VRMS % Error	Maximum AZRMS % Error	Error Ratio
Modulus	390 / 2.7	4.7	4.5	1.03
Damping	729 / 5.0	8.7	8.7	1.00
Density	1220 / 8.4	14.6	4.3	3.40
Length	1034 / 7.1	12.4	9.9	1.26

3.3 Case 3: Combined Beam Random Vibration

Analysis on a two-material, combined beam was performed in the same manner as the cantilever beam, with a few modifications. For the input loading, the ASD frequency range is changed to 100 to 3000 Hz and the input location is moved to the bottom of the beam, in between the two joined sections (blocks), as shown in **Fig. 10**. The loading direction is kept the same- in the positive Z direction. Also, two points are used to probe the acceleration and stress for each block, for a total of four points in the combined beam model. These points are placed at the top of the blocks to study results in a different location than Case 2.

The combined beam model is the same overall length and mesh size as the cantilever beam, and the two blocks are joined together, with the material properties defined independently. The model is half steel, half aluminum, with equivalenced nodes at the interface to provide an ideal joint. The perturbation is performed similarly to the previous problem, except that the modulus, density, and length are only changed for the aluminum beam. For the perturbed length model, the length of the aluminum beam was increased by 0.125 inches (3.2 mm) for each simulation and the point coordinates were unchanged.

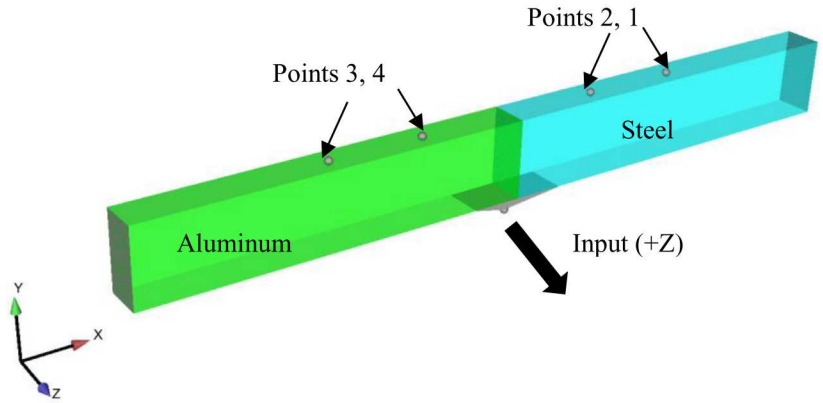

Fig. 10 Combined Beam Model with Coordinate System, Input, and Point Location for the Two Sections

The response ASD for the base model is shown in **Fig. 11**. There are several modes across the frequency range, many of which are close in frequency. Two of the modes that produce the highest response are also shown in **Fig. 11**.

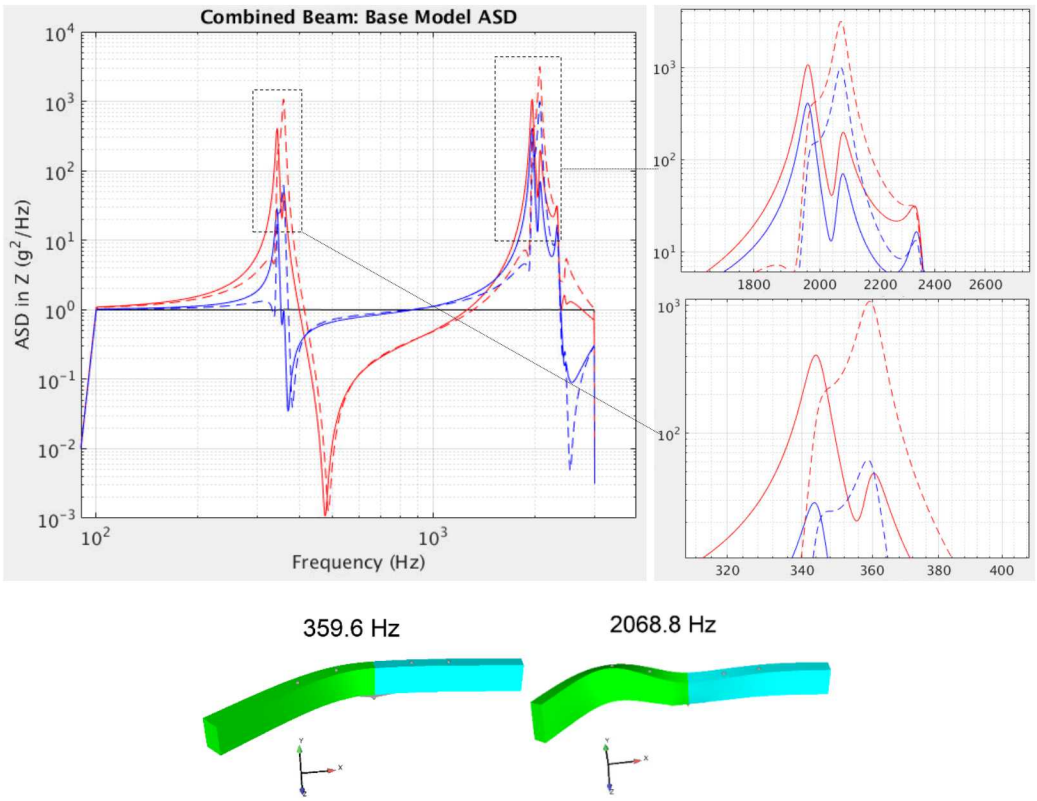

Fig. 11 Combined Beam: Base Model ASD and Modes with Highest Response

Examining the results for the modulus perturbation in **Fig. 12**, the general trends are like those from the cantilever beam problem. However, the error relation is clearly nonlinear. For the change in damping, a linear relationship similar to the cantilever beam was observed, although it was not one-to-one for the maximum; the plots are given in Appendix B. For the density and length perturbations, the results were much more unpredictable than the previous example. The error plots for the density change in **Fig. 13** are nonlinear and inconsistent, with several turning points, although some sections appear uniform. The error results for the length perturbation shown in **Fig. 14** are also erratic.

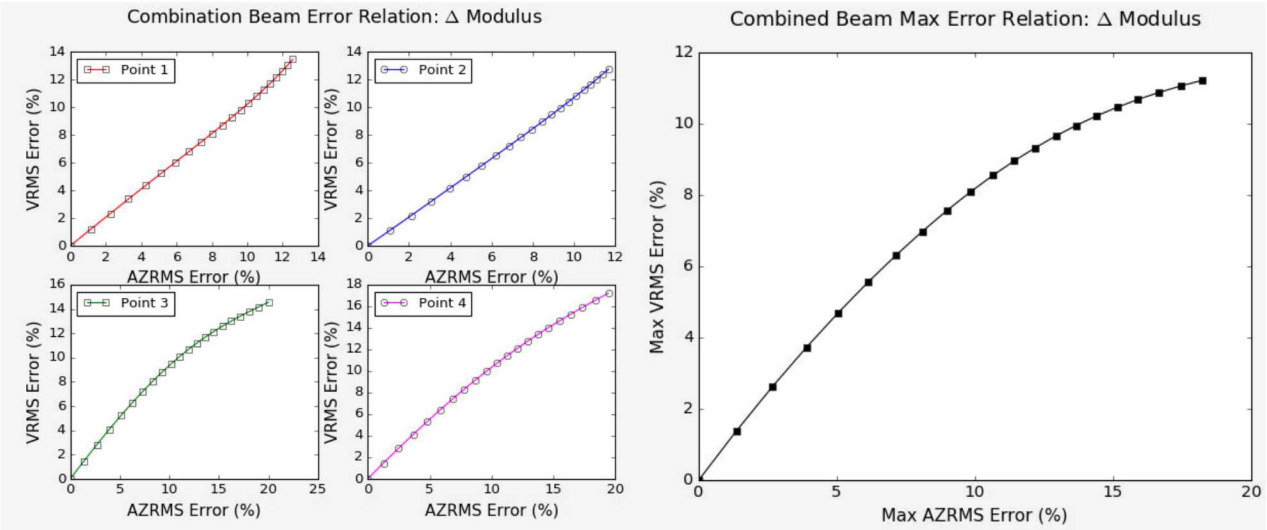

Fig. 12 Combined Beam: Effect of Modulus Change on Stress-Acceleration Error Relation, Selected Points and Maximum

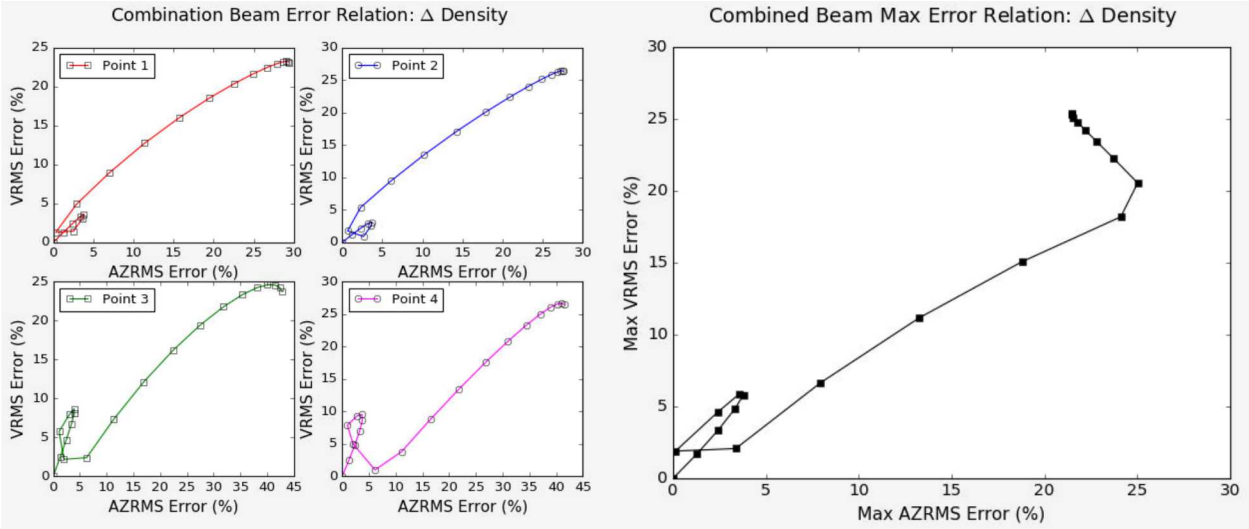

Fig. 13 Combined Beam: Effect of Density Change on Stress-Acceleration Error Relation, Selected Points and Maximum

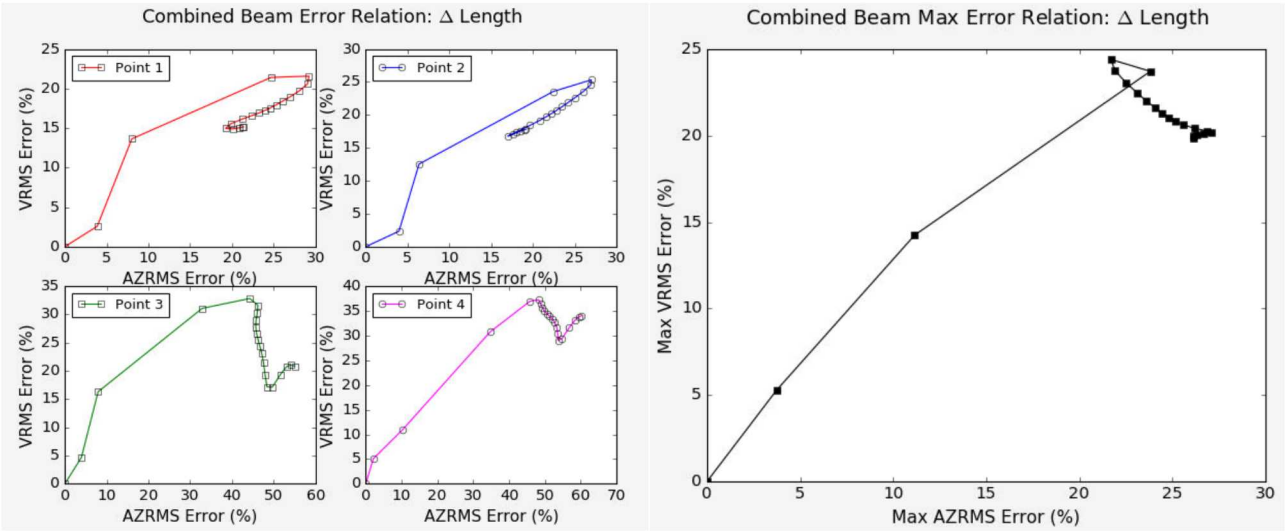

Fig. 14 Combined Beam: Effect of Length Change on Stress-Acceleration Error Relation, Selected Points and Maximum

As in the previous example, the response ASD is studied to determine the source of the inconsistency between stress error and acceleration error. **Fig. 15** shows the ASD at Point 1 for each simulation in the modulus perturbation study. The modes change gradually as the modulus changes and no new modes enter the input frequency range, but the large variation in response could contribute to the nonlinearity of the plots in **Fig. 12**.

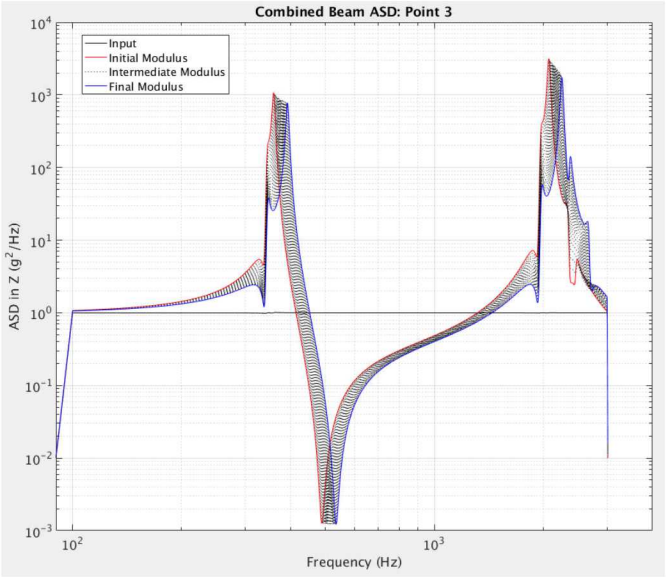

Fig. 15 Combined Beam: Complete Range of Response ASD for Modulus Perturbations

Next, we examine possible reasons for the unpredictable error relation presented earlier. In **Fig. 14**, there is a large AZRMS error caused by a 1% perturbation in length. From the 2nd to the 3rd perturbed model, an increase in length of 0.125 inch (3.2 mm) resulted in a 15% change in acceleration error and almost a 10% change in maximum stress error. These changes are apparent in the ASD, in **Fig. 16**. The peak acceleration response nearly doubled at 2 kHz for Point 3. Additionally, two modes near 350 Hz are nearly indistinguishable before the small change in length, yet clearly distinct after the small increase in length. These abrupt changes had a substantial impact on the resulting error relationship.

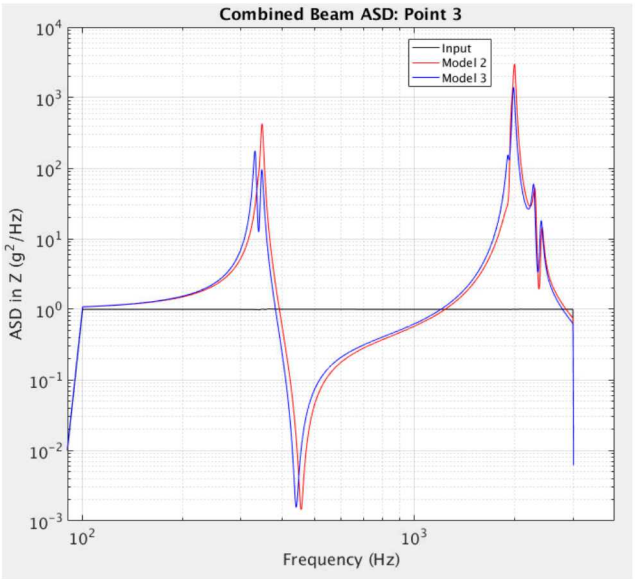

Fig. 16 Combined Beam: Model 1 and 2 Response ASD for Length Perturbations

Furthermore, some parts of the error relationship were consistent, such as models 9 through 12 of the length perturbation study, shown in **Fig. 17**. This can be attributed to the lack of new modes introduced to the input load frequency range, illustrated in the **Fig. 18** ASD. The response over models 9 through 12 is relatively stable, which is contrasted by the drastic change in the response over the entire perturbation range.

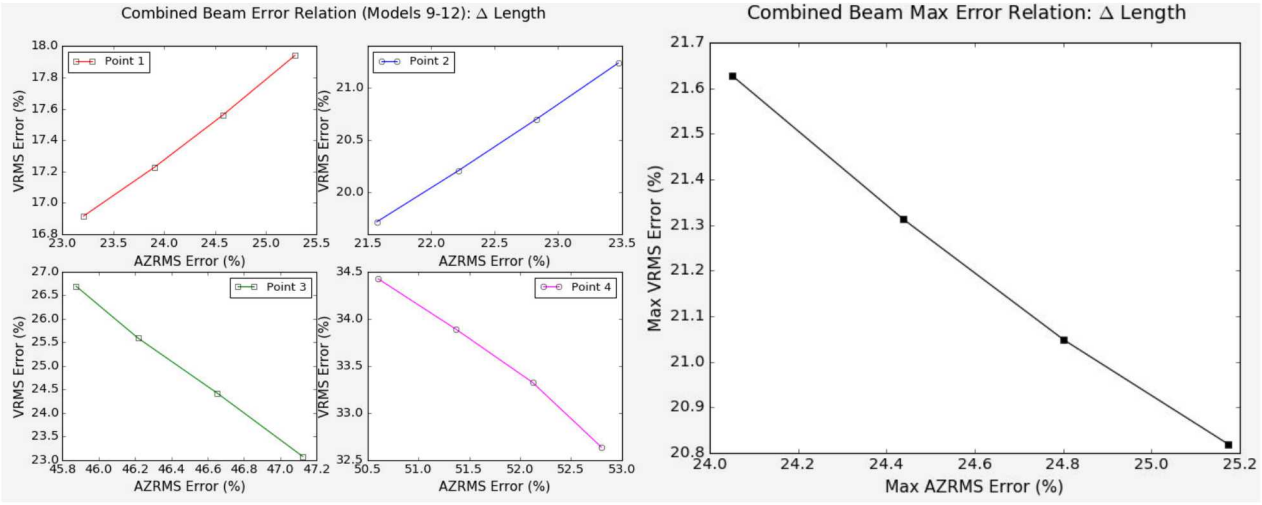

Fig. 17 Combined Beam: Effect of Length Change on Stress-Acceleration Error Relation (Models 9 through 12)

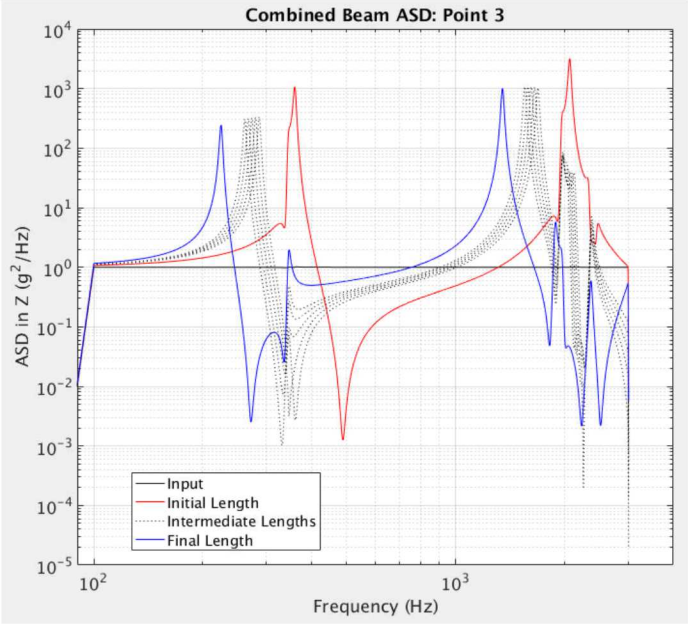

Fig. 18 Combined Beam: Models 9 through 12 and Range of Response ASD for Length Perturbations

Although many of the results obtained from this combined beam example were not as straightforward as the previous two cases, the error ratio still gives an idea of the observed limits of stress and acceleration error. For the density and length studies, the error ratio is omitted since the inconsistent trends make it an inadequate measure of the error bound. A summary of the maximum value results is given in **Table 2.**

Table 2 Combined Beam: Maximum Value Error Summary

Perturbation	VRMS Range (psi / MPa)	Maximum VRMS % Error	Maximum AZRMS % Error	Error Ratio
Modulus	1767 / 12.2	8.2	18.2	0.45
Damping	2304 / 15.9	7.8	9.9	0.79
Density	13960 / 96.3	25.4	25.0	-
Length	13250 / 91.4	24.4	27.1	-

4 EVALUATION

The data suggests that in an ideal case, a linear relationship between the stress error and acceleration error should be expected. However, as uncertainties in model parameters cause the system modes to change significantly, the results can vary greatly and it becomes difficult to quantify the error relationship.

Case 1 presents a theoretical linear relationship between the error in maximum modal von Mises stress and acceleration. As a practical extension of this initial study, Case 2 and 3 demonstrate a similar relationship for random vibration simulations. Results show that there can be large changes in the stress error and acceleration error if the mode shapes are significantly affected by a relatively small change in properties. These perturbations can have a pronounced effect if modes are close in frequency, and the error relation can become unpredictable.

For the random vibration examples, a change in damping exhibited the only consistently linear error relationship, with a direct relationship between VRMS and AZRMS error at each point, although the error ratio was not necessarily 1 over the model maximum. Still, this direct relationship is to be expected since uniform modal damping was specified. As for the range of errors, over the 20% perturbation in each model parameter, the highest stress error was 25.4 % for the density and length perturbation in Case 3. In addition, the highest error ratio observed was 3.4, for the cantilever beam density perturbation. The error ratio is a useful measure for the cantilever beam, but it is specific to the system and model parameter and may have limitations if the model increases in complexity, or if measurements are made at stress concentrations or near boundary conditions. Additionally, a low error in acceleration does not necessarily correspond to a low error in stress, since it depends on the modes of the system being stable and predictable.

More data is needed to see how results hold for more complex systems, and future work could include multiaxial inputs, input load uncertainty, and coupled parametric effects. It would also be interesting to study results from other modal-based analyses, such as a modal transient solution to see if a bound could be determined even if the modal stress is not directly used.

5 CONCLUSION

A relationship between the error in stress and acceleration was calculated for three example problems. For the first case, a linear relation and theoretical bound for the maximum modal von Mises stress error and acceleration error was determined. The results were extended to a random vibration solution that utilized the modal stress and two example cases were considered. An error in acceleration due to changes in modulus of elasticity, damping ratio, density, and length for each example beam was related to the error in VRMS stress. An error ratio was defined to describe and bound the relationship and results were found to be linear if the system mode shapes do not change significantly with perturbation in model parameters. Irregular behavior was observed when new modes were introduced into the input load frequency range, influencing the response between perturbed models. The results of this work support that, given the stability of system modes across uncertainty in model parameters, the error in stress could be related to and bound through the errors in acceleration for a random vibration analysis. These error trends are a useful starting point for providing a quantitative measure of accuracy in stress and acceleration predictions.

REFERENCES

[1] Christie, M.A., Glimm, J., Grove, J.W., Higdon, D.M., Sharp, D.H., and Wood-Schultz, M.M., “Error analysis and simulations of complex phenomena”, *Los Alamos Science*, Vol. 29, pp 6-25.

[2] Segalman, D.J., Fulcher, C.W.G., Reese, G.M., and Field Jr., R.V., “An Efficient Method for Calculating RMS. von Mises Stress in a Random Vibration Environment,” *Journal of Sound and Vibration,* Vol. 230, No. 2, 2000, pp. 393-410.

[3] Clough, R., and Penzien, J., *Dynamics of Structures*, 2nd ed., Rev., Computers and Structures, Inc., Berkeley, California, 2010.

[4] Wirsching, P.H., Paez, T.L., and Ortiz, K., *Random Vibrations: Theory and Practice*, Dover Publications, Inc., Mineola, New York, 2006.

APPENDICES

APPENDIX A

This section includes further explanation of the theory discussed in 2.1. Additional details on the nonlinear equation to be solved, $\|\ddot{u}_h - P\ddot{u}_H\|_{L^2}^2$, are also presented. If the approximations are accurate, the solution is not difficult. As the acceleration grows however, larger bounds on the stress mist be computed carefully.

At some time, t, the error is given as

$$\|\ddot{u}_h - P\ddot{u}_H\|_{L^2}^2 = \langle\, \Phi^h\ddot{q} - P\,\Phi^H\ddot{b}, \Phi^h\ddot{q} - P\,\Phi^H\ddot{b}\rangle_M \tag{A1}$$

Introducing the matrices

$$T = \phi^T P^T M P\phi, \qquad B = \phi^T P^T M P\phi^h \tag{A2}$$

There holds

$$\|\ddot{u}_h - P\ddot{u}_H\|_{L^2}^2 = \ddot{q}^T\ddot{q} - 2\ddot{b}^T B\ddot{q} + \ddot{b}^T T\ddot{b} \tag{A3}$$

Note that B and T are identity matrices if the modes are exact. An alternative to the acceleration problem is the displacement problem, involving

$$\|u_h - Pu_H\|_{L^2}^2 = q^T q - 2b^T Bq + b^T Tb \tag{A4}$$

For the displacement problem, Ω^h is omitted from the definition of X. For the acceleration problem, q, b, c are replaced by $\ddot{q}, \ddot{b}$ and $\ddot{c}$ respectively. Setting c as

$$c = B^T b \tag{A5}$$

The goal is to establish sufficient conditions for $q^T X\, q \approx c^T Xc$. And setting

$$\beta = \sqrt{b^T Tb} \tag{A6}$$

Next comes the second assumption about how typically the nonlinear equations are easy to solve. We can expect $\beta \geq \|c\|$, but for clarity we assume $\beta \geq \|c\|$.

$$q^T q - 2b^T Bq + b^T Tb = q^T q - 2c^T q + \beta^2 = \|q - c\|^2 + \beta^2 - \|c\|^2 \tag{A7}$$

The case of interest is the case in which q cannot have rotated around from c all the way to the eigenvectors of X with large eigenvalues.

A Lagrangian for this problem is $L(q,\lambda) = \frac{1}{2}q^T Xq - \frac{1}{2}\lambda(q^T q - 2q^T c + c^T c)$, the critical points satisfy $Xq = (q - c)\lambda$.

Two definitions are included for clarification. First let $\delta_{min} = (\beta^2 - \|c\|^2)^{1/2}$. And second, let $\bar{\delta} = \sqrt{\delta^2 - \delta_{min}^2}$.

To determine the Lagrange multiplier, first solve for q, and then eliminate q from the constraint equations,

$$q = (\lambda - X)^{-1}c\lambda, \qquad \|(\lambda - X)^{-1}Xc\| = \bar{\delta} \tag{A8}$$

Equation (A8) must be solved for λ. The value of the Lagrange multiplier is not unique. The equation $Xq = (q - c)\lambda$ implies that $\|Xq\| = \bar{\delta}|\lambda|$ So, in practice the maximum corresponds to the largest positive Lagrange multiplier, $\lambda > \|X\|$. However, in general this would have to be another assumption. We assume that $\lambda_{max}(X) = \|X\|$.

There is a case in which an approximate solution is obvious. Suppose that $\tau = \|Xc\|/\delta \gg \|X\|$. In this case $(\tau - X)^{-1} \sim \tau^{-1}$ and $\lambda \sim \tau$. For sufficiently small δ, $\lambda \sim |Xc|/\delta$ and $\lambda > \|X\|$. A more precise statement involves $\gamma \geq 1$ defined by $\|Xc\| = \|X\|\|c\|\gamma$.

It turns out that if $\delta < \gamma\|c\|$, then $\lambda \sim \|Xc\|/\delta$. This is seen by manipulating the equation $\tau = \|Xc\|/\delta \geq \|X\|$. First using the definition of γ, $\|X\|\|c\|\gamma/\delta > \|X\|$. Next, $\|X\|$ is cancelled, leaving $\|c\|\gamma/\delta > 1$ or $\|c\|\gamma > \delta$.

This means that the estimated value of λ can be used instead of the exact value and that $q \sim c$, which is the benign case. This is to be expected, since usually the approximation is quite accurate and the nonlinear equation is trivial to solve.

Typically, $\gamma \ll 1$. On the other hand, if $\delta > \|c\|\gamma$, then it is worthwhile to carefully solve the nonlinear equation that determines λ; we expect that $\|a\| \sim \bar{\delta}$.

APPENDIX B

This section includes the stress-acceleration error plots omitted from the main text.

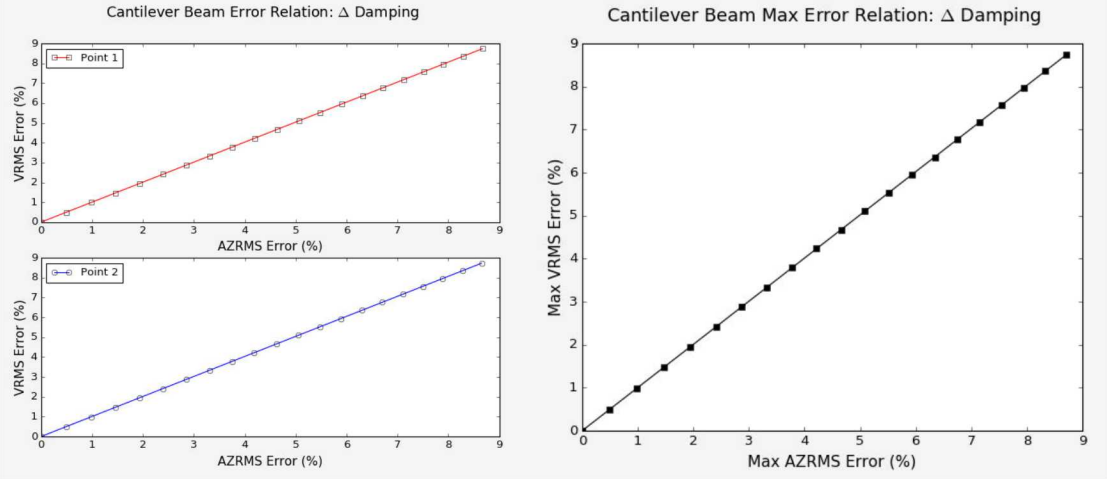

Fig. B1 Cantilever Beam: Effect of Damping Change on Stress-Acceleration Error Relation, Selected Points and Maximum

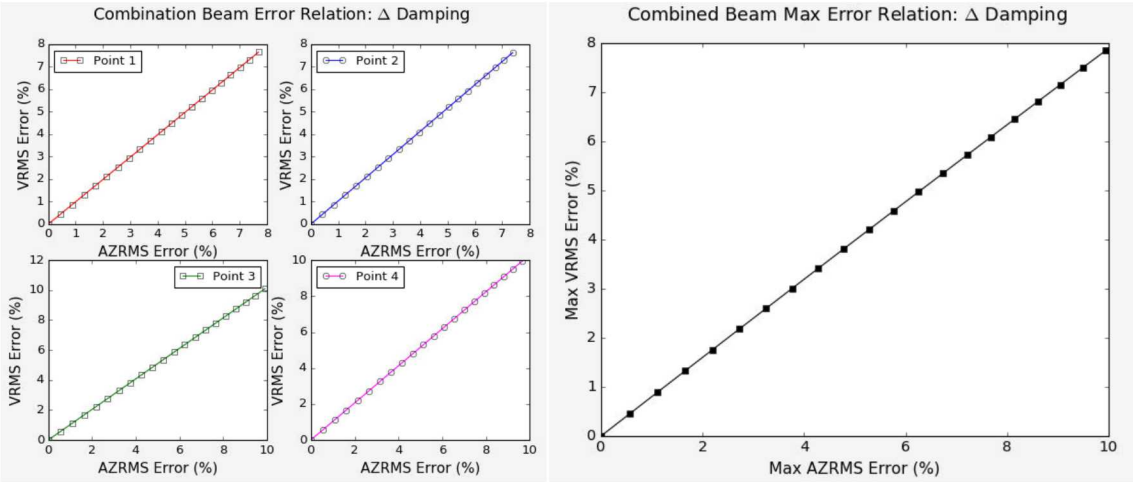

Fig. B2 Combined Beam: Effect of Damping Change on Stress-Acceleration Error Relation, Selected Points and Maximum